Optimized Control Based on Nonlinear Modelling and Parameter Estimation of the Electro-Hydraulic Servo System

Optimized Control Based on Nonlinear Modelling and Parameter Estimation of the Electro-Hydraulic Servo System

Meng Li[1] and Yong Zhang[1]

[1] National Engineering Laboratory for Automotive Electronic Control Technology, Shanghai Jiao Tong University, No.800, Rd. Dongchuan, Minhang, Shanghai, China

lemon_lee@sjtu.edu.cn

Abstract. In this paper, a nonlinear physical model of the electro-hydraulic system is built and described in Bond Graph in order to show its physical structure and flow of energy. The nonlinear model is simplified based on response bandwidth of different parts of system and nonlinear degree. A series of typical parameters of the model are chosen based on the effect on nonlinear response of system and estimated with the experiment response. A simple and useful model based nonlinear feedforward PID control methods is proposed based on the steady state response of system and dynamic stribeck friction force. The simulation and experiment results of parameter estimation and feedforward control are presented, which shows that the model response with estimated parameters can fit the experimental data very well, and the simulation and experiment response of the optimized control can eliminate the nonlinear response very well. Therefore, the nonlinear model and control method used in this paper have a guiding significance and application value, and have theory value for the further research of hydraulic servo system with the similar structure.

Key words: electro-hydraulic, Bond Graph, nonlinear model, stribeck friction, parameter estimation, feedforward PID.

1. Introduction

Because of its operation characteristics, the displacement servo system for the automotive vibration test equipment should have the capability of large load, large movement, high accuracy, fast response and long time working stability[1-3]. Electro-hydraulic system fits the requirements and has advantages on cost and reliability; therefore, it is widely used in vibration test equipment[4, 5]. The dual-nozzle force feedback two-stage electro-hydraulic servo valve and the symmetric hydraulic actuator are commonly used in electro-hydraulic servo system[6, 7].

The physical principles of hydraulic system and hydraulic components have been well researched[8, 9]. For the servo valve, from the first beginning many kinds of linear model have been developed, like the 2-order model which only contains the main valve dynamic characteristic[10-14], the 3-order model which adds the 1 order torque motor model[8, 14]. In order to get more accurate results, higher order model including linear and nonlinear model is necessary, like 5-order servo valve model which adds 1 order torque motor and 2-order pilot valve[15, 16], 5-order servo valve which adds 2-order torque motor and 1 order pilot valve[14], 7-order model which adds 2-order torque motor, 2-order pilot valve and 1-order nozzle output pressure feedback[17]. For hydraulic actuator, it also has many kinds of model, like 2-order model which mostly represents actuator's piston moving characteristics[18, 19], 4-order actuator which contains 2-order compression and 2-order piston

kinematic[13, 20], the multi-body model with stribeck friction model[21], the thermal-hydraulic model based on the electro-hydrostatic theory[22].

Generally speaking, when the model has higher order, it will get higher simulation accuracy, better dynamic characteristics and be closer to the real equipment, while at the same time, it will get less stability and need higher calculation capacity. Considering the needs of the vibration test and combined with the actual characteristics of equipment and predecessors' experience, the order and structure of model in this paper are determined.

This paper can be divided into 4 parts. Firstly, the nonlinear model is structural analysed with Bond Graph and described as simultaneous differential equations, especially the nonlinear elements like hydraulic flow, valve opening and stribeck friction[23]; And the nonlinear model is simplified base on the frequency bandwidth of different parts of the system, so the main valve flow and whole actuator which have smallest bandwidth and effect the system output mostly are remain. Secondly, based on the simplified model, a series of parameter including characteristics of the main valve flow and actuator motion that hard to measure and important to system response are chosen and estimated with experiment response. Thirdly, based on the system steady state transfer characteristics, the control method of the damping and stribeck friction feedforward is proposed. Finally, the results of sine wave response with initial and estimated parameters as well as original PID[24, 25] and model based feedforward PID control are presented.

2. Nonlinear model

2.1. *Structure*

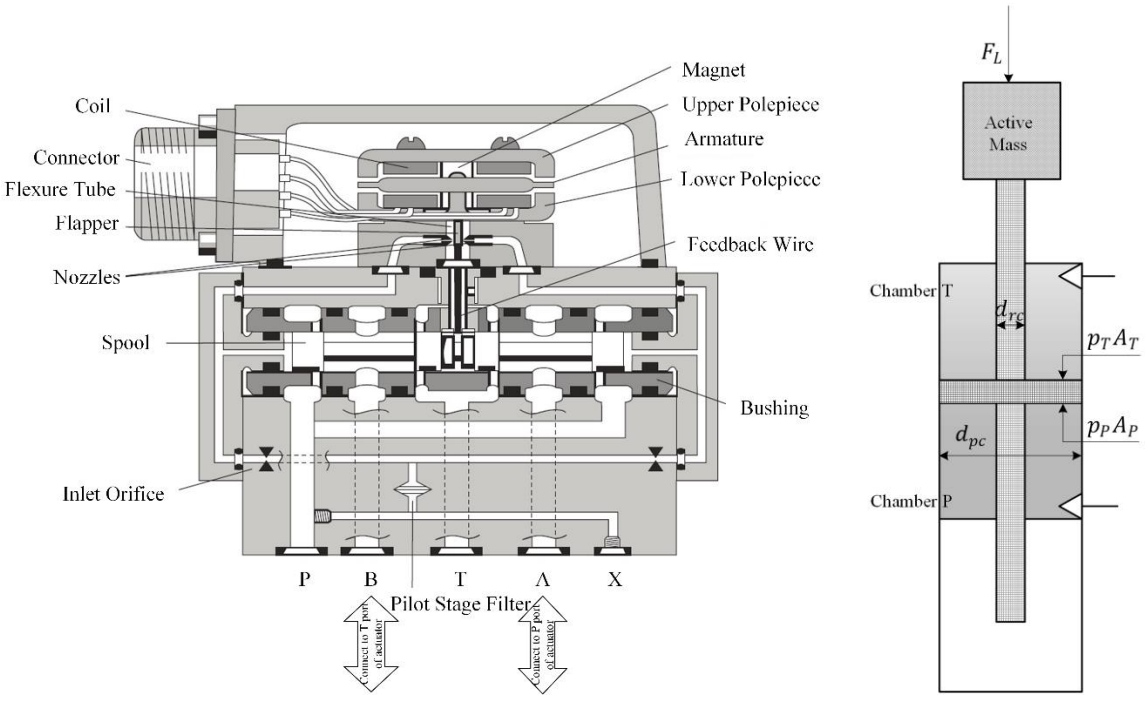

Figure 1 Electro-hydraulic servo valve and actuator profile[26]

In the figure 1, it's the profile of the MOOG G761 series servo valve, and is force feedback 2 stage electro-hydraulic servo valve. Its pilot valve is dual-nozzle flapper valve, which driven by permanent magnet moving-iron torque motor. Its main valve is 4-way spool valve, and valve core's displacement is connected to armature of the torque motor by feedback wire, to constitute force feedback loop of spool valve.

As you can see, the actuator is a symmetric actuator, so we set chamber on the bottom side as the Chamber P, the other side as Chamber T. The pressure force difference between two active chambers will make the piston move.

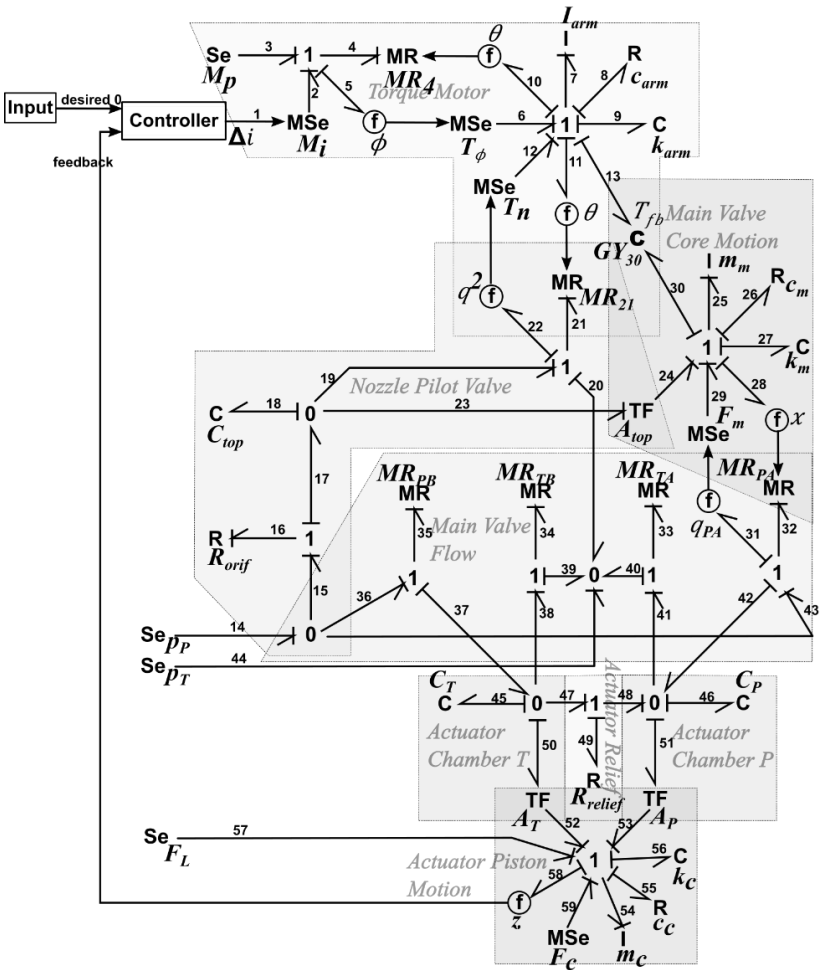

Figure 2 System bond graph, for the sake of observation, the magnetic air gap of the torque motor in the diagram has only one quadrant, the pilot valve only has the left half, and the fluid forces of the main valve only contain PA valve port.

As shown in the figure 2, the inputs of controller are the desired displacement (node 0) and feedback displacement (node 58) of the actuator, and the output of controller is the servo current (node 1) that inputted into the servo valve;

The servo valve contains torque motor, pilot valve and main valve;

The actuator contains two compression chambers and the piston;

The 0 junction connected with the nodes 14,15,36 and 43 represents the chamber of oil supply, while the 0 junction connected with the nodes 20,39,40 and 44 represents the chamber of oil return flow;

2.2. *Full model*

The full model is the summary of the nonlinear model, which written as:

$$\dot{\boldsymbol{x}} = f(\boldsymbol{x}, \boldsymbol{u}), \boldsymbol{y} = H\boldsymbol{x} \tag{1}$$

The vector of independent variables $\boldsymbol{x}$, inputs $\boldsymbol{u}$ and outputs $\boldsymbol{y}$ are:

$$\boldsymbol{x} = [\dot{\theta} \quad \theta \quad p_{t,L} \quad p_{t,R} \quad \dot{x} \quad x \quad p_{CP} \quad p_{CT} \quad \dot{z} \quad z]^{\mathrm{T}}, \boldsymbol{u} = [\Delta i \quad F_L]^{\mathrm{T}}, \boldsymbol{y} = [z] \tag{2}$$

The variables $\boldsymbol{x}$ contains the rotational speed $\dot{\theta}$ and angle θ of torque motor, the pressure of left $p_{t,L}$ and right $p_{t,R}$ chambers of pilot valve, the speed $\dot{x}$ and displacement x of the main valve, the

pressure of P p_{CP} and T p_{CT} chambers of the actuator, as well as the speed $\dot{z}$ and displacement z of the piston of the actuator.

The differential equations are

$$f=\begin{cases} \mathrm{I}_7\ddot{\theta}+\mathrm{R}_8\dot{\theta}+\mathrm{K}_\theta\theta=\mathrm{K}_{\Delta i}\Delta i+\mathrm{MSe}_{12}[q^2_{n,L|(\theta,p_{t,L})}-q^2_{n,R|(\theta,p_{t,R})}]+\mathrm{GY}_{13}x \\ \dot{p}_{t,L}=\mathrm{C}_{18}q_{L|(\theta,p_{t,L})}-\mathrm{C}_{18}\mathrm{TF}_{23}\dot{x} \\ \dot{p}_{t,R}=\mathrm{C}_{18}q_{R|(\theta,p_{t,R})}+\mathrm{C}_{18}\mathrm{TF}_{23}\dot{x} \\ \mathrm{I}_{25}\ddot{x}+\mathrm{R}_{26}\dot{x}+(\mathrm{C}_{27}+\mathrm{GY}_{30})x=\mathrm{TF}_{24}p_{t,L}-\mathrm{TF}_{24}p_{t,R}+\mathrm{GY}_{30}l_{fb}\theta+F_{m|(\dot{x},x,p_{CP},p_{CT})} \\ \dot{p}_{CP}+\mathrm{K}_\mathrm{C}p_{CP}=\mathrm{C}_{46}q_{P|(x,p_{CP})}+\mathrm{K}_\mathrm{C}p_{CT}-\mathrm{TF}_{50}\dot{z} \\ \dot{p}_{CT}+\mathrm{K}_\mathrm{C}p_{CT}=\mathrm{C}_{46}q_{T|(x,p_{CT})}+\mathrm{K}_\mathrm{C}p_{CP}+\mathrm{TF}_{50}\dot{z} \\ \mathrm{I}_{54}\ddot{z}+\mathrm{R}_{55}\dot{z}+\mathrm{C}_{56}z=\mathrm{TF}_{52}p_{CP}-\mathrm{TF}_{52}p_{CT}+F_L+F_{c|(\dot{z})} \end{cases} \tag{3}$$

The f contains 7 differential equations, which respectively represent armature swing, pressure of the left and right chambers of pilot valve, main valve moving, pressure of the P and T chambers of actuator, and actuator piston moving.

2.3. *Simplified Model*

Because the relationship between input current and the displacement response of value core of the servo valve is nearly linear, and its bandwidth is much larger than the cylinder response.

So the system can be simplified as:

$$\dot{\boldsymbol{x}}_s=\tilde{f}(\boldsymbol{x_s},\boldsymbol{u}),\boldsymbol{y}=\tilde{H}\boldsymbol{x_s} \tag{4}$$

The vector of simplified independent variables $\boldsymbol{x_s}$, inputs $\boldsymbol{u}$ and outputs $\boldsymbol{y}$ are:

$$\boldsymbol{x_s}=[p_{CP}\quad p_{CT}\quad \dot{z}\quad z]^\mathrm{T},\boldsymbol{u}=[\Delta i\quad F_L]^\mathrm{T},\boldsymbol{y}=[z] \tag{5}$$

The expressions of simplified model are:

$$\tilde{f}=\begin{cases} x\cong\mathrm{K}_x\Delta i \\ \dot{p}_{CP}\cong\mathrm{C}_{46}\mathrm{K}_q x-\mathrm{TF}_{50}\dot{z} \\ \dot{p}_{CT}\cong-\mathrm{C}_{46}\mathrm{K}_q x+\mathrm{TF}_{50}\dot{z} \\ \mathrm{I}_{54}\ddot{z}+\mathrm{R}_{55}\dot{z}+\mathrm{C}_{56}z=\mathrm{TF}_{52}(p_{CP}-p_{CT})+F_L+F_{c|(\dot{z})} \end{cases} \tag{6}$$

The K_C which represents leakage of the actuator is ignored, and the flow of main value to the cylinder chambers is linearized at the balance point of the system when the input is zero, as shown below:

$$q_P\cong\mathrm{K}_q x\,,q_T\cong-\mathrm{K}_q x \tag{7}$$

where the K_q the linearized flow coefficient of the valve opening, at the actuator's pressure balance point, which the leak is ignored and pressure is stable:

$$\mathrm{K}_q=C_d\pi(d_s+d_c/2)\sqrt{\rho_{oil}(p_P-p_T)} \tag{8}$$

3. Parameter Estimation

In the parameter analysis, the sine signal is chosen because the response is highly nonlinear and the features are easy to observe. The input signal is sine signal of 0 mean, 0.04m amplitude and 1Hz frequency.

3.1. *Parameter choosing*

The main valve opening parameters discussed in this paper include: valve core-seat gap d_c, valve core edge round radius r_c, and valve opening bias x_{bias}, which affect main valve flow. These parameters in the main valve is hard to measure, by the same time, they have great influence on the nonlinear characteristics of the response, so these parameters need to be discussed.

The actuator parameters discussed in this paper include: actuator coulomb force F_{cc}, actuator strict friction force F_{sc}, actuator inactive length l_{iac}, actuator damping c_c.

In practical use, the friction and damping coefficients will vary greatly with environmental parameters, oil deterioration and equipment wear. In addition, although stroke of the hydraulic

cylinder can be measured, but connecting path between the servo valve and the hydraulic cylinder is very complex, at the same time, the hydraulic cylinder seal stiffness is much smaller than the piston and cylinder block itself, and it is difficult to measure.

3.2. *Estimation*

The cost function chosen in this paper for the parameter estimation is sum absolute error (SAE). The optimization method used to estimate the parameter is nonlinear least squares[27], and the algorithm is trust region reflective[28].

The iteration process is shown in the figure 3 below:

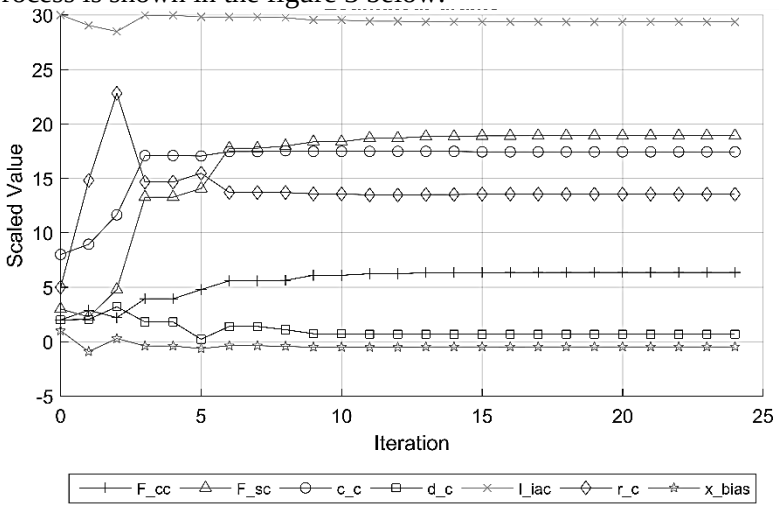

Figure 3 Estimation iteration

After 24 times of iteration for the parameter estimation, the parameters tend to be stable. The values in the **Figure 3** are scaled by the 'Scale gain' in the **Table 1** to distinguish values more clearly.

The initial, boundary and estimated value of the parameters are shown in the table 1 below:

Table 1 Estimated parameters

Parameter	Initial value	Boundary value	Estimated value	Scale gain	Dimension
$\boldsymbol{d_c}$	1×10-6	[1×10-6, +∞)	8.4918×10-6	5×10-7	m
$\boldsymbol{r_c}$	1×10-6	[1×10-7, +∞)	1.5238×10-6	2×10-7	m
$\boldsymbol{x_{bias}}$	1×10-6	[-6×10-6, 6×10-6]	-3.6659×10-8	1×10-6	m
$\boldsymbol{F_{cc}}$	200	[50, +∞)	1.0469×103	100	N
$\boldsymbol{F_{sc}}$	300	[100, +∞)	2.2019×103	100	N
$\boldsymbol{l_{iac}}$	0.15	[0.105, +∞)	1.4417×10-1	0.005	m
$\boldsymbol{c_c}$	8000	[2000, +∞)	1.610×104	1000	Ns/m

The time responses with initial and estimated parameters are shown in figure 5 and figure 6.

4. Control method

The sketch of the control is shown in the figure 4 below:

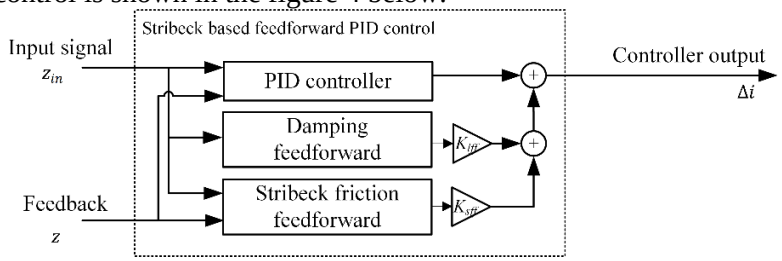

Figure 4 Controller sketch

The controller contains PID controller, damping feed forward and stribeck friction feed forward.

4.1. *Feedforward*

When the time of force is short, then the movement of cylinder piston could be ignored, so the pressure function of the chambers of the cylinder can be simplified as:

$$\dot{p}_{CP} - \dot{p}_{CT} = 2\mathrm{C}_{46}\mathrm{K}_q x \tag{9}$$

Therefore, the steady state gain between the integration of the input current and the hydraulic pressure force on the cylinder piston is:

$$\mathrm{K}_p = 2\mathrm{TF}_{52}\mathrm{C}_{46}\mathrm{K}_q\mathrm{K}_x \tag{10}$$

Which means the steady state hydraulic pressure force on the cylinder piston is

$$F_p = \mathrm{K}_p \int \Delta i \, \mathrm{d}t \tag{11}$$

The stribeck force and the damping force should be counteract by the feedforward pressure force, as shown below:

$$F_{psc} = -F_c + c_{visc}\dot{z} \tag{12}$$

Therefore, the feedforward compensation is:

$$\Delta i_{sc} = \frac{1}{2\mathrm{TF}_{52}\mathrm{C}_{46}\mathrm{K}_q\mathrm{K}_x}\frac{\mathrm{d}F_{psc}}{\mathrm{d}t} \tag{13}$$

4.2. *Stribeck estimation*

For the feedforward control, the stribeck force needs to be estimated. The stribeck friction is a function of speed and resultant force of the cylinder piston,

$$F_c = f_c(\dot{z}, F_{oc}) \approx -\left[\left(1 - \xi_{fc}\right)\mathrm{saturation}(F_{oc}, -F_{sc}, F_{sc}) + \xi_{fc}\mathrm{sign}(\dot{z})\, F_{cc}\right] \tag{14}$$

where the ξ_{fc} is stribeck transition between column force and steady state friction force,

$$\xi_{fc} = [\tanh(\mathrm{abs}(\dot{z})/v_c - 1) + 1]/2 \tag{15}$$

and the F_{oc} is the resultant force of the actuator except the friction force. If do not consider the load force, the resultant force is pressure force as expressed in (12).

So the stribeck friction force is:

$$F_c = f_c(\dot{z}, F_{oc}) \cong f_c(\dot{z}, F_p) \tag{16}$$

4.3. *Delay between signal and response*

Generally, the delay between signal and response is constant, and can be expressed as:

$$z = e^{-\tau s} z_{in} \tag{17}$$

where the τ is delay time, z_{in} is input signal.

For feedforward control, the response is unknown, and can be replaced by delayed input signal if the delay can be measured.

4.4. *Control method summery*

The control output of the controller is the summery of PID output and feedforward:

$$\Delta i = \mathrm{PID}(z - z_{in}) + \Delta i_{sc} \tag{18}$$

where the PID() is:

$$\mathrm{PID}(\Delta z) = K_p \Delta z + K_i \int \Delta z \mathrm{d}t + K_d \frac{\mathrm{d}\Delta z}{\mathrm{d}t} \tag{19}$$

and the feedforward output is:

$$\Delta i_{sc} = \frac{1}{2\mathrm{TF}_{52}\mathrm{C}_{46}\mathrm{K}_q\mathrm{K}_x}\frac{\mathrm{d}}{\mathrm{d}t}\left[-f_c\left(e^{-\tau s}\dot{z}, \mathrm{K}_p \int \Delta i \, \mathrm{d}t\right) + c_{visc} e^{-\tau s}\dot{z}\right] \tag{20}$$

5. Results

5.1. *Test Settings*

For vibration and fatigue test equipment, sine signal is often used, so it is chosen as input signal.

The input is sine signal of 0 mean, 0.04m amplitude and 1Hz frequency.

In order to observe the contrast between the responses and the input signal, the simulation and experiment curve are translated by -0.016s. The PID parameters for the simulation and experiment are [0.75 0.051 0.00049] which separately are the gain of proportion, integration and derivation.

5.2. *Response with initial and estimated parameters*

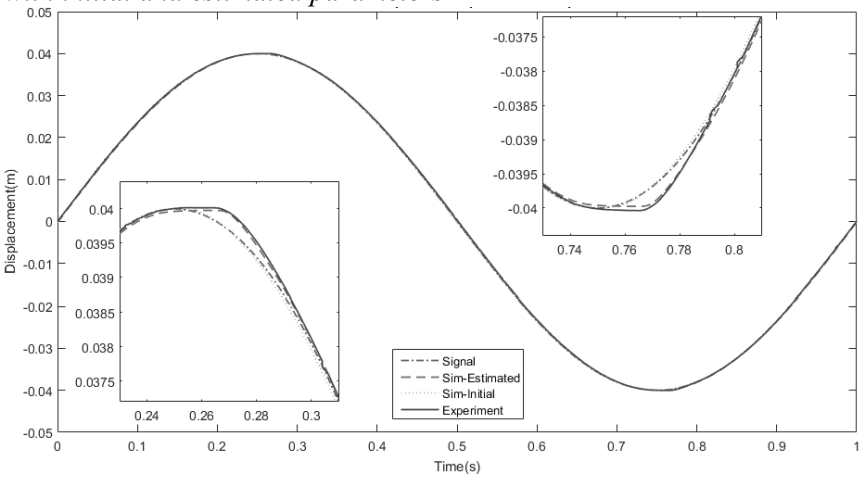

Figure 5 Actuator displacement response with initial and estimated parameters

As shown in figure 5, the displacement response of the experiment has ceiling phenomenon; the simulation response with initial parameter is very close to signal but different from the experiment response, while the simulation response with estimated parameter is close to the experiment results.

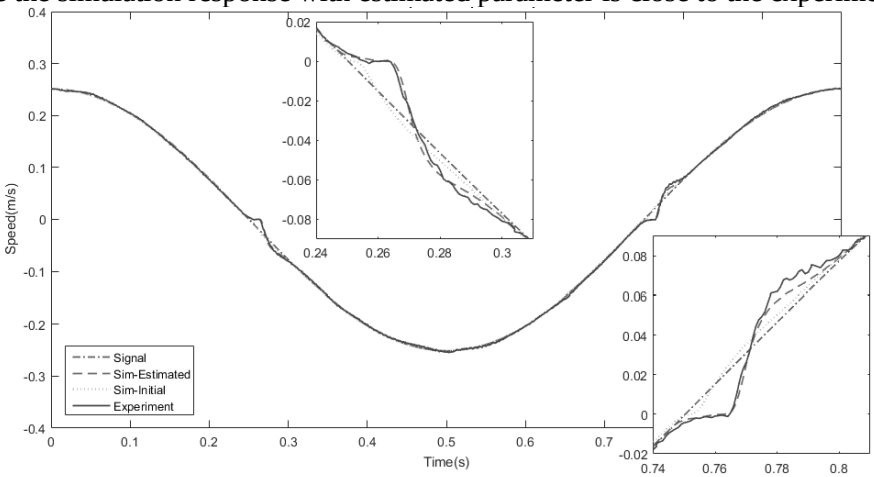

Figure 6 Actuator speed response with initial and estimated parameters

As shown in figure 6, the speed response of the experiment has dead-zone phenomenon; the dead-zone phenomenon of the simulation response with initial parameters is very small, while the simulation response with estimated parameter is close to the experiment.

5.3. *Response with PID and feed forward PID controller*

The simulation responses with PID and feedforward PID controller are shown in the figure 7 below:

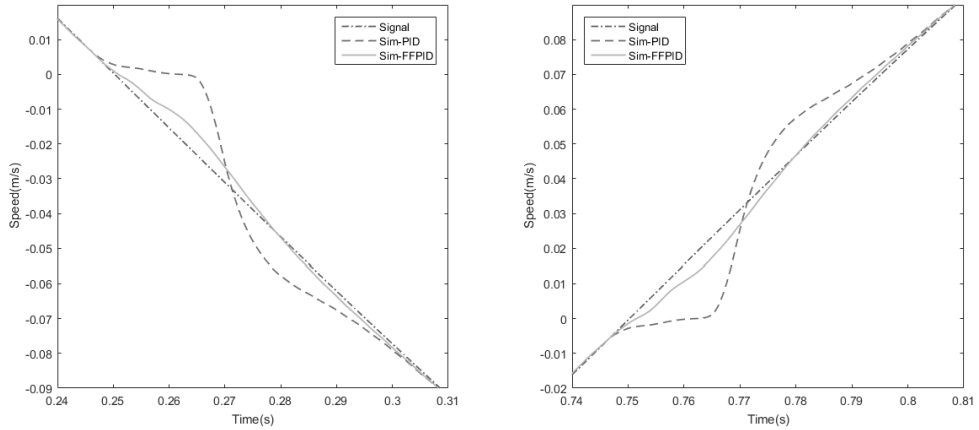

Figure 7 PID and FFPID Simulation Speed Response

The experiment response of system with PID and feedforward PID controller are shown in the figure 8 below:

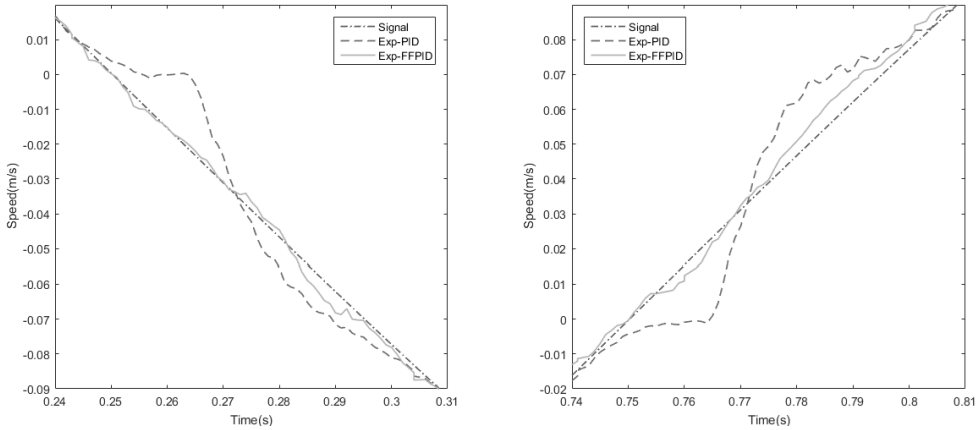

Figure 8 PID and FFPID Experiment Speed Response

As shown in the figure 7 and figure 8, the responses of feed forward (FF) PID of both simulation and experiment are better than the normal PID, and the nonlinear dead-zone phenomenon of the response near the zero point is much smaller.

5.4. *Discussion*

The results of simulation and experiment shows that the model can accurately describe the actual equipment, and after parameter estimation, the response of simulation is close to the experiment results. Because of the stribeck friction of actuator piston, displacement tracking has ceiling phenomenon and speed tracking has dead-zone phenomenon. When the input is small, the hydraulic drive force of actuator is very small. After actuator stops moving, it needs to overcome static friction force that is bigger than sliding friction to start moving again.

As shown in the results, the nonlinear response with initial parameters is very different from the experiment, and the response with estimated parameters is close to the experiment, which means the parameter estimation is usable.

With the estimated parameters and the stribeck friction feed forward, the nonlinear dead-zone phenomenon of the response is much smaller than the original PID control. Though the feedforward PID control cannot fully eliminate the nonlinear characteristics, because the steady state assumption of the feedforward controller. However, considering computation requirement and availability on the actual test bench, the feedforward controller in this paper is valuable and useful.

6. Conclusion

In this paper, the physical structure and energy flow of the typical hydraulic servo system are described in the Bond Graph, and with the graph, a 10 order nonlinear physical model are built. The nonlinear elements mainly include the flow nonlinearity of the valve port, the nonlinear opening of the valve, and the stribeck nonlinear friction of the hydraulic actuator.

The nonlinear model is simplified based on the difference of the frequency response bandwidth of the servo valve and actuator. Some parameters of the simplified model that are important and hard to measure are estimated based on the speed response of the experiment. The simulation and experiment results of estimation and feedforward control is presented.

To sum up, in this paper, and a high order nonlinear hydraulic servo model is set up, and is consistent with actual situation. The model response with estimated parameters can fit the experimental data very well, and the simulation and experiment response of the optimized control can eliminate the nonlinear response very well. Therefore, the nonlinear model and control method used in this paper have a guiding significance and application value, and have theory value for the further research of hydraulic servo system with the similar structure.

7. Declaration on conflict of interest

The authors declare that there is no conflict of interests regarding the publication of this article.

References

[1] P. Xu, D. Wong, P. LeBlanc, and G. Peticca, "Road Test Simulation Technology in Light Vehicle Development and Durability Evaluation," in *2005 SAE World Congress* Detroit, Michigan: SAE International, 2005, p. 12.

[2] C. J. Dodds and A. R. Plummer, "Laboratory Road Simulation for Full Vehicle Testing: A Review," in *Symposium on International Automotive Technology 2001*: SAE International, 2001, pp. 487-494.

[3] B. Cryer, P. Nawrocki and R. Lund, "A Road Simulation System for Heavy Duty Vehicles," in *SAE Technical Paper* 1976 Automotive Engineering Congress and Exposition: SAE International, 1976.

[4] A. Akers, *Hydraulic power system analysis*. Boca Raton, Fla.: Boca Raton, Fla. : CRC/Taylor & Francis, 2006.

[5] D. Van Den Bossche, "The A380 flight control electrohydrostatic actuators, achievements and lessons learnt," in *25th international congress of the aeronautical sciences*, 2006, pp. 1-8.

[6] M. Inc., "Electrohydraulic Valves... A Technical Look,". vol. 2018, 2018.

[7] F. Yeaple, "Hydraulic and Electrohydraulic Cylinders and Actuators," in *Fluid Power Design Handbook* New York: Marcel Dekker, Inc., 1995, pp. 111-115.

[8] H. E. Merritt, *Hydraulic control systems*. New York: John Wiley and Sons, Inc., 1967.

[9] J. Wang, H. Zhang and Y. Huang, *Hydraulic and Pneumatic Transmission*, 2 ed. Beijing: China Machine Press, 2005.

[10] S. Zhou, X. Cao and Y. Cen, "Optimal Control of Speed Conversion of a Valve Controlled Cylinder System," *Journal of Dynamic Systems, Measurement, and Control,* vol. 113, pp. 691-695, 1991-12-01 1991.

[11] J. T. William, *Transfer functions for moog servovalves*. New York: Moog Controls Division, 1965.

[12] K. Dasgupta, J. Watton and S. Pan, "Open-loop dynamic performance of a servo-valve controlled motor transmission system with pump loading using steady-state characteristics," *Mechanism and Machine Theory,* vol. 41, pp. 262-282, 2006-01-01 2006.

[13] M. Kalyoncu and M. Haydim, "Mathematical modelling and fuzzy logic based position control of an electrohydraulic servosystem with internal leakage," *Mechatronics,* vol. 19, pp. 847-858, 2009-01-01 2009.

[14] G. Jacazio and L. Borello, "Mathematical Modelling and Analysis for the Air Force," *Mathematical Computational Modelling,* vol. 11, pp. 563-569, 1988.

[15] D. H. Kim and T. Tsao, "A Linearized Electrohydraulic Servovalve Model for Valve Dynamics Sensitivity Analysis and Control System Design," *Journal of Dynamic Systems, Measurement, and Control,* vol. 122, pp. 179-187, 1998-02-02 1998.
[16] D. H. Kim and T. Tsao, "An improved linearized model for electrohydraulic servovalves and its usage for robust performance control system design," in *Proceedings of the 1997 American Control Conference*. vol. 6 Albuquerque, New Mexico, 1997, pp. 3807-3808.
[17] C. Liu and H. Jiang, "A seventh-order model for dynamic response of an electro-hydraulic servo valve," *Chinese Journal of Aeronautics,* vol. 27, pp. 1605-1611, 2014-01-01 2014.
[18] N. Hori, A. S. Pannala, P. R. Ukrainetz, and P. N. Nikiforuk, "Design of an Electrohydraulic Positioning System Using a Novel Model Reference Control Scheme," *Journal of Dynamic Systems, Measurement, and Control,* vol. 111, pp. 292-298, 1989-06-01 1989.
[19] S. R. Lee and K. Srinivasan, "Self-Tuning Control Application to Closed-Loop Servohydraulic Material Testing," *Journal of Dynamic Systems, Measurement, and Control,* vol. 112, pp. 680-689, 1990-12-01 1990.
[20] D. Sha, V. B. Bajic and H. Yang, "New model and sliding mode control of hydraulic elevator velocity tracking system," *Simulation Practice and Theory,* vol. 9, pp. 365-385, 2002-01-01 2002.
[21] A. Ylinen, H. Marjamäki and J. Mäkinen, "A hydraulic cylinder model for multibody simulations," *Computers and Structures,* vol. 138, pp. 62-72, 2014-01-01 2014.
[22] K. Li, Z. Lv, K. Lu, and P. Yu, "Thermal-hydraulic Modeling and Simulation of the Hydraulic System based on the Electro-hydrostatic Actuator," *Procedia Engineering,* vol. 80, pp. 272-281, 2014-01-01 2014.
[23] M. Woydt and R. Wäsche, "The history of the Stribeck curve and ball bearing steels: The role of Adolf Martens," *Wear,* vol. 268, pp. 1542-1546, 2010-01-01 2010.
[24] K. M. Elbayomy, J. Zongxia and Z. Huaqing, "PID Controller Optimization by GA and Its Performances on the Electro-hydraulic Servo Control System," *Chinese Journal of Aeronautics,* vol. 21, pp. 378-384, 2008-01-01 2008.
[25] K. J. Åström and T. Hägglund, "The future of PID control," *Control Engineering Practice,* vol. 9, pp. 1163-1175, 2001-01-01 2001.
[26] M. Inc., "Servo Valves Pilot Operated Flow Control Valve with Analog Interface G761/761 Series, Size 04,", 2004.
[27] Jr. J. E. Dennis, *"Nonlinear Least-Squares." State of the Art in Numerical Analysis*: Academic Press.
[28] T. F. Coleman and Y. Li, "An Interior Trust Region Approach for Nonlinear Minimization Subject to Bounds," *SIAM Journal on Optimization,* vol. 6, pp. 418-445, 1996-05-01 1996.